# Combined Molecular Mechanics (MM2) and Molecular Orbital (AM1) Study of Periplanone-A and Analogues. Evaluation of Biological Activity from Electronic Properties and Geometries. Part 2†

**Kazuko Shimazaki,*[,a] Masataka Mori,[a] Kentaro Okada,[a,‡] Tatsuji Chuman,[a,‡] Shigefumi Kuwahara,[b,§] Takeshi Kitahara,[b] Kenji Mori,[b] Hitoshi Gotō,[c] Eiji Ōsawa,[c] Kazuhisa Sakakibara[d] and Minoru Hirota[d]**

[a] *Life Science Research Laboratory, Japan Tobacco Inc., 6-2 Umegaoka, Midori-ku, Yokohama 227, Japan*

[b] *Department of Agricultural Chemistry, Faculty of Agriculture, The University of Tokyo, 1-1-1 Yayoi, Bunkyo-ku, Tokyo 113, Japan*

[c] *Department of Knowledge-based Information Engineering, Toyohashi University of Technology, 1-1 Hibarigaoka, Tempakucho, Toyohashi 441, Japan*

[d] *Department of Synthetic Chemistry, Faculty of Engineering, Yokohama National University, 156 Tokiwadai, Hodogaya-ku, Yokohama 240, Japan*

Combined molecular mechanics (MM) and semiempirical molecular orbital (MO) calculations have been applied to periplanone-A (**1**), the epoxy epimer (**2**) and a structurally-related analogue (**3**). Conformational properties of these compounds have been obtained by the use of MM2 with an additional set of force-field parameters in conjunction with an automatic conformation generating program. The global minimum **1A** has the same type of ring conformation as that found in periplanone-B (**4**). The remarkable contrast between **1** and **4** is the presence in **1** of significant amounts of conformers having different ring conformations such as **1B**. In both **2** and **3**, which are far less biologically active than **1**, **1A** ring type conformers exist only in low populations. The conformer distribution of **2** obtained by MM2 well explains the highly complex NMR (2D-NOESY) spectrum. The MM-predicted geometries of the stable conformers of **3** show good agreement with that observed in dynamic NMR spectroscopy. When the **1B** ring type conformers are taken into account, the accuracy of the previously proposed index for the evaluation of the pheromone activity of analogues, effective frontier parameter $EF^{(N)}_{(S)}$, is improved.

Periplanones-A (P–A, **1**),¶[1,2] and -B (P–B, **4**)[3,4] are the sex pheromone components of the American cockroach (*Periplaneta americana* L.). Their unique structural features and

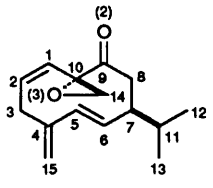

Periplanone-A **1**

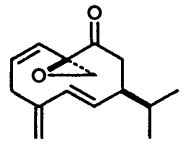

Epoxy epimer **2**

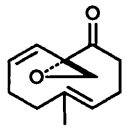

Analogue **3**

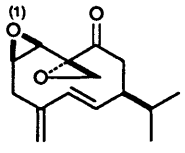

Periplanone-B **4**

potent biological activity (threshold: $10^{-11}$ g for **1**; $10^{-13}$ g for **4**, assessed by behavioural tests)[5] have attracted much attention from many organic chemists. To reveal the structural requirements for the biological activity of periplanones, we have been studying the conformational and electronic properties of these pheromones by a combination of X-ray analyses, NMR measurements, MM and MO calculations[6,7] and bioassay.[5] MM analysis on the periplanone-type compounds was made possible by the development of additional force field parameters and by the new program CONFLEX2 which exhaustively generates low energy conformers. In our previous paper, we described how the biological activities of P–B (**4**) and some structurally-related analogues (**5**–**8**) depended closely on the total population of conformers having the same ring conformation as the global minimum of **4** and on their frontier unoccupied molecular orbital localized around the upper part of the ten-membered ring, abbreviated to '$FUMO_{upper}$'.[7] Since the ring conformation and molecular orbital ($FUMO_{upper}$) found in the global minimum of the most biologically active P–B (**4**) could be regarded as the biologically relevant ones, we proposed a new index for the prediction of biological activity of periplanone-analogues, called effective frontier parameter $EF^{(N)}_{(S)}$. It includes the contribution of the electron density and orbital energy in $FUMO_{upper}$ of all of the stable conformers and the ring structure of biologically important conformers. $EF^{(N)}_{(S)}$ is defined as shown in eqns. (1)–(3).

$$f_r^{(N)} = 2C^2_{r(FUMO_{upper})} \quad (1)$$

$$Ef_r^{(N)}{}_{(S)} = \Sigma\{f_r^{(N)}\mu/E_{(FUMO_{upper})\mu}\} \times Pop\mu \times A \qquad \mu = 1\text{-}M \quad (2)$$

$$EF^{(N)}_{(S)} = \Sigma\{Ef_r^{(N)}{}_{(S)}\} \quad r = 1\text{-}R \quad (3)$$

where, $f_r^{(N)}$ is the frontier electron density in $FUMO_{upper}$ of

† Part 1: see ref. 7.

‡ *Present address:* Head Office, Japan Tobacco Inc., 4-12-62 Higashi-shinagawa, Shinagawa-ku, Tokyo 140, Japan.

§ *Present address:* Laboratory of Agricultural Chemicals, Faculty of Agriculture, Ibaraki University, 3998 Ami-machi, Inashiki-gun, Ibaraki 300-03, Japan.

¶ The same numbering scheme for the carbon atoms as has been used for **1** by Persoons *et al.*[3] is employed in this paper.

**Table 1** Newly developed force-field parameters for vinyl-epoxy compounds

(*a*) Bending parameters

| Angle type | kb/mdyn Å rad$^{-2}$ | $\theta_0$/deg |
|---|---|---|
| <2–73[a]–49[b] | 0.883 | 117.167 |
| <2–73–3 | 0.499 | 117.300 |

(*b*) Torsional parameters

| Dihedral angle type | V1 | V2 | V3 |
|---|---|---|---|
| 2–2–73–49 | 0.088 | 3.044 | −1.392 |
| 5–2–73–49 | 0.000 | 0.000 | 0.010 |
| 2–73–49–73 | −0.160 | −0.260 | 0.140 |
| 2–73–73–49 | −0.186 | −0.180 | 0.432 |
| 2–73–49–20 | 0.000 | 0.000 | 0.000 |
| 1–2–2–73 | −0.740 | 12.812 | 0.736 |
| 2–2–73–3 | −0.602 | 1.170 | 0.286 |
| 5–2–73–3 | 0.604 | 1.148 | −0.296 |
| 2–73–3–7 | −1.460 | 0.436 | 0.188 |
| 2–73–3–1 | 1.494 | 0.450 | −0.282 |

[a] The atom type of epoxide carbon atom for MM calculation. [b] The atom type of epoxide oxygen atom for MM calculation.

atom *r*, *r* is the atom number (excepting protons), *R* is the total number of atoms considered, $\mu$ is the number of local minima, *M* is the total number of local minima, $E_{FUMO_{upper}}$ is the frontier orbital energy of $FUMO_{upper}$ (eV), Pop is the population of each local minimum at 25 °C, and *A* is the structure factor: 1, the ring conformation is well superimposable on that of global minimum of **4**; 0, the conformation is not superimposable. The biological activity and $EF^{(N)}_{(S)}$ of P–B (**4**) and compounds **5–8** showed a good linear relation as in eqn. (4).

$$\log_{10}[\text{Activity threshold (g)}] = -3.844 - 2.104 \times EF^{(N)}_{(S)} \quad (4)$$

($R = 0.929$, $\sigma = 1.35$, $F = 18.89$, SE = 0.48, $t_{static} = 4.35$ and $n = 5$).[7]

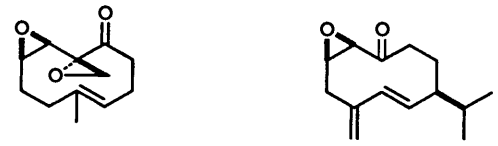

**5** **6**

**7** Germacrene D **8**

Another natural pheromone P–A was first isolated and characterized along with P–B by Persoons *et al.* in 1974.[3] However, because of the very minute amount and instability of the isolated sample, the structural elucidation remained unsettled for a long time. In 1986, Hauptmann *et al.* independently isolated P–A from female American cockroach and proved synthetic **1** to have high pheromone activity.[1] The epoxy epimer (**2**) has also been proposed to be the structure of P–A by Macdonald.[8] Recently, the structure of P–A has been established to be **1** by the synthesis of both **1** and **2**, coupled with the X-ray crystallographic analysis of **1**.[2] The bioassay of **2** shows a drastic reduction of the biological activity (threshold: $10^{-7}$ g).[5,6] In the meantime, a structurally-simplified analogue (**3**) was synthesized with the expectation of strong biological activity by analogy with the highly active analogue **5** (threshold: $10^{-9}$ g), but **3** showed no significant biological activity even at a dose of $10^{-5}$ g.[5]

The reduction of the biological activities of **1**, **2** and **3** from that of **4** is considered to be due to changes in steric and electronic factors. Thus, it was deemed valuable to reveal these properties of **1**, **2** and **3** for the improvement of structure–activity relationship. Although the X-ray and NMR data had been reported, data on the conformational properties of these compounds remained scarce.[6] An MM study on **1** has been reported, but the results are unreliable due to the lack of force-field parameters for the vinyl-epoxy group.[9]

In this study, the quantitative evaluation of the conformer distribution of **1**, **2** and **3** has been performed by MM calculations with newly developed force-field parameters, and the electronic properties of the stable conformers calculated with a semiempirical molecular orbital (AM1) method.[10] On the basis of this information, we discuss structural characteristics of **1**, **2** and **3** by comparison with those of P–B and analogues, and examine the validity of $EF^{(N)}_{(S)}$ as an index to evaluate their pheromone activity in comparison with their experimental bioassay.

## Experimental

Preparation and characterization of compounds **1–3** have been described previously.[6,11] Their biological activities were assessed by behavioural tests.[5]

*Computational Details.—Force-field parameters.* New parameters for vinyl-epoxy functional group were estimated by fitting to the results of *ab initio* calculations using GAUSSIAN 90[12] on model compounds 2-vinyloxirane (**A**), 2-allyoxirane (**B**) and 2-acetyl-2-vinyloxirane (**C**) at the MP2/6-31G*//HF/6-31G* level on an IBM power station R6000/550.[13] A new parameter set is summarized in Table 1. The relative energies of stable conformers obtained by *ab initio* and by MM2 methods are shown in Fig. 1.

MM2 program, version '87, was obtained from Molecular Design Ltd.[14] All possible ring conformations were generated by CONFLEX[15,16] and optimized by MM2. The Boltzmann population of each energy minimum at 25 °C was calculated on the basis of its steric energy. Average vicinal H/H coupling constants ($J_{HH}$'s) were calculated from 60 energy minima of **1** and 64 of **2** using Altona's empirical modification of the Karplus equation.[17–19] The optimized geometries of conformers having populations above 1.0% obtained by CONFLEX/MM2 calculations were used as the input for AM1 (AMPAC version 2.1)[10] calculations. The total number of the stable conformers calculated are seven for **1**, 12 for **2**, and three for **3**. These MM and MO calculations were carried out on an IRIS 4D/320GTX workstation (Silicon Graphics). Three-dimensional structures, frontier orbital extension and superposition of the target molecules were visualized by the use of QUANTA (Molecular Simulations Inc., USA).

*NMR Measurements.*—$^1$H NMR (500 MHz) spectra were measured at 27 °C on a Bruker AM-500 instrument with $Me_4Si$ as internal standard. The NMR data for **1** and **2** recorded in $C_6D_6$ solutions have been described in our previous paper.[6] In this study, $CDCl_3$ was employed for the solvent, in view of the better resolution of signals. The spectrum lines of **3** broadened

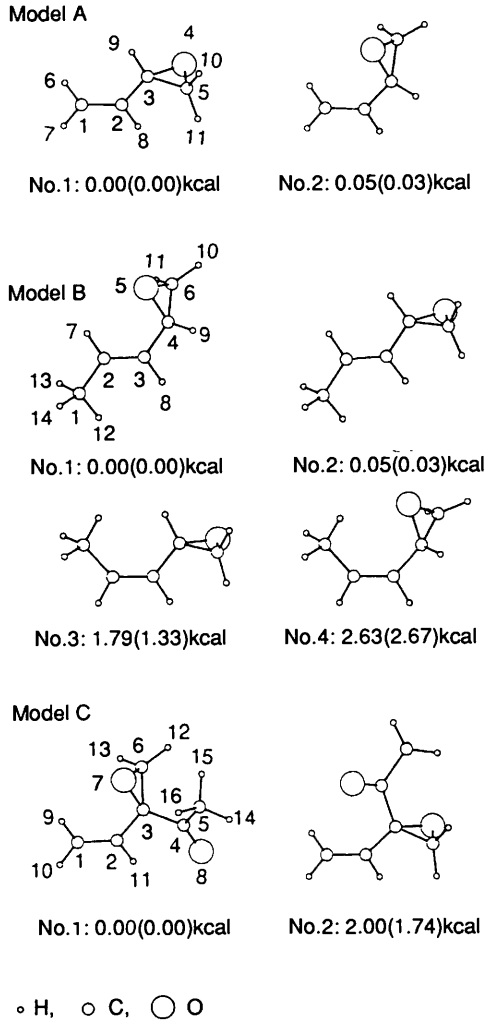


**Fig. 1** Stable conformers of model compounds calculated by *ab initio* (MP2/6-31G*//HF/6-31G*) and their relative energies (MM2 values in parentheses)

remarkably at normal temperature. For the estimation of $T_1$ values (inversion recovery method) and the measurement of the 2D-NOESY spectrum of **2**, Bruker standard software (version: 870 101.0) was employed. Dynamic NMR measurement on **3** was carried out in $CD_2Cl_2$ solution with the same instrumentation under cooling with $N_2$ stream. DNMR measurements on **1** and **2** did not give well-resolved spectra, presumably owing to the decrease in the solubility of the compounds at lower temperatures. *J*-Values are given in Hz. $^1$H NMR spectral data for **1** in $CDCl_3$ are identical to those reported by Hauptmann *et al.*[1] For **2**: $\delta_H$(500 MHz, in $CDCl_3$ at 300 K) 6.00 (1 H, d, *J* 11.0, H-1, $T_1$ = 3.13 s), 5.86 (1 H, d, *J* 16.2, H-5, $T_1$ = 2.78), 5.67 (1 H, dt, *J* 11.0, 8.1, H-2, $T_1$ = 2.66), 5.62 (1 H, dd, *J* 9.6, 16.2, H-6, $T_1$ = 2.25), 4.94 (1 H, br s, H-15, $T_1$ = 1.52), 4.81 (1 H, t, *J* 1.5, H-15', $T_1$ = 1.63), 3.13 (1 H, dd, *J* 12.5, 8.8, H-3α, $T_1$ = 1.24), 3.08 (1 H, d, *J* 6.6, H-14, $T_1$ = 1.52), 2.90 (1 H, dd, *J* 12.5, 8.1, H-3β, $T_1$ = 1.59), 2.89 (1 H, d, *J* 6.6, H-14', $T_1$ = 1.08), 2.56 (1 H, dd, *J* 11.0, 5.9, H-8α, $T_1$ = 1.08), 2.51 (1 H, dd, *J* 11.0, 8.1, H-8β, $T_1$ = 1.01), 2.27 (1 H, m, H-7, $T_1$ = 1.81), 1.68 (1 H, m, H-11, $T_1$ = 1.80), 0.96 (3 H, d, *J* 6.6, H-12, $T_1$ = 1.01), 0.91 (3 H, d, *J* 6.6, H-13, $T_1$ = 1.01). For **3**: $\delta_H$(500 MHz, in $CDCl_3$, at 300 K) 6.06 (1 H, d, *J* 11.0, H-1), 5.79 (1 H, dt, *J* 7.1, 11.0, H-2), 5.43 (1 H, br, H-6), 2.85 (1 H, d, *J* 6.0, spiroepoxy), 2.8 (1 H, m, H-3), 2.79 (1 H, d, *J* 6.0, spiroepoxy), 2.78 (1 H, m, H-8), 2.48 (1 H, br, H-7), 2.35 (1 H, br, H-7'), 2.28 (1 H, br, H-4), 2.1 (1 H, br, H-8'), 2.03 (1 H, m, H-3'), 1.74 (1 H, dt, *J* 3.1, 12.7, H-4'), 1.57 (3 H, s, methyl group at C-5).

## Results and Discussion

*Molecular Mechanics Calculations.*—The conformational properties of major conformers having over 4% Boltzmann populations at 25 °C of **1**, **2** and **3** are summarized in Tables 2, 3 and 4, respectively.

*Periplanone-A* (**1**). CONFLEX2 generated 60 energy minima. Among them, six major conformers of **1** (**1A** to **1F**) within 1.2 kcal mol$^{-1}$ from the global energy minimum are considered significant, and they are shown in Fig. 2.* Only two types of ring conformations appear in these major conformers, each containing three rotamers at the isopropyl groups in addition to those depicted in Fig. 2. **1A**, **1D**, and **1F** have almost identical twist-chair (TC) ring conformations, in spite of the distinction of their nomenclatures.[20] The structure of global minimum **1A** can be considered identical with the X-ray structure (Table 2).[6] It should be noted that the ring conformation **1A**, and also **1D** and **1F**, is the same as the global minimum of **4**. The combined population of these conformers, **1A**, **1D** and **1F** amounts to 48.7%. On the other hand, the second stable conformer **1B**, as well as the rotamers **1C** and **1E**, have a ring structure in which the C(2)–C(3)–C(4)–C(5) portion including the C(4) *exo*-methylene group flap upward. The dihedral angle of C(15)–C(4)–C(5)–C(6) in **1B** (−55.5°) is about 100° different from that of **1A** (*ca.* −151.5°). As can be seen in Fig. 3, **1A** and **1B** are almost superimposable except for the *exo*-methylene moiety. Flapping of the *exo*-methylene group brings epoxy-oxygen [O(3)] close to the C(5)–C(6) moiety in **1B** [O(3)–C(5) = 3.00 Å , O(3)–C(6) = 2.86 Å], in comparison with **1A** [O(3)–C(5) = 3.82 Å, O(3)–C(6) = 3.05 Å]. The calculated vicinal H/H coupling constants ($^3J_{HH}$'s) essentially agree with those observed [7–8a: obs. 11.8 (*J*/Hz), calc. 12.08 (*J*/Hz); 7–8β: obs. 5.2 (*J*/Hz), calc. 3.27 (*J*/Hz)].

*Epoxy epimer* (**2**). Four conformers of **2** are considered significant (Fig. 4). The ring conformation of global minimum **2A** has never appeared in our previous studies, while those of **2B** and **2D** are similar to that of **1A** (Table 3). The difference of the ring conformation between **2A** and **2C** can be seen along C(7)–C(8)–C(9)–C(10) moiety, where the flap around the carbonyl group causes H-1 to approach H-8β (2.68 Å). These results are consistent with the NMR data. The complex 2D-NOESY spectrum[6] of **2** (Fig. 5) indicates the coexistence of two or more conformers. This spectrum contrasts with that of **1** where only three NOE contacts (H-5/H-7, H-5/H-15, H-6/H-3) involving H-5 and H-6 could be measured.[6] The observed NOE contacts can be explained in terms of the three major conformers. The assignments of the NOESY cross peaks and proximate proton pairs in each conformer of **2** are shown in Fig. 6. The calculated vicinal H/H coupling constants ($^3J_{HH}$'s) essentially agree with those observed [7–8α: obs. 5.9 (*J*/Hz), calc. 4.62 (*J*/Hz); 7–8β: obs. 8.1 (*J*/Hz), calc. 7.87 (*J*/Hz)].

*Analogue* (**3**). The CONFLEX/MM analysis identified three important conformers for **3**, which are shown in Table 4 and Fig. 7. In contrast to the bio-active analogue **5** which has the same ring conformation as that of global minimum **4**, the global minimum **3A** possesses a quite different conformation from that of **1**. The second stable conformer (**3B**), which occupied 32.6% population at 25 °C, has the same ring conformation to those of both **1A** and the global minimum of **5**. At room temperature, the broadened $^1$H NMR spectrum of **3** produced no coupling and NOE data for the sp$^3$ protons were obtained. Dynamic

* 1 cal = 4.184 J.

**Table 2** Conformational properties of **1** and X-ray data of **1**.

| | 1A | 1B | 1C | 1D | 1E | 1F | X-Ray[a] |
|---|---|---|---|---|---|---|---|
| Ring conformation[b] | [123'1'3'] | [14'1'4'] | [14'1'4'] | [124'3'] | [14'1'4'] | [124'3'] | [123'1'3'] |
| $\Delta E_S$/kcal mol$^{-1}$ | 0.0 | 0.14 | 0.50 | 0.63 | 1.09 | 1.11 | |
| Boltzmann dist. (%) at 25 °C | 32.5 | 25.8 | 14.0 | 11.2 | 5.2 | 5.0 | |
| Dihedral angle/° | | | | | | | |
| C(10)–C(1)–C(2)–C(3) | −7.5 | −3.2 | −3.3 | −7.7 | −3.2 | −7.6 | −3.5 |
| C(1)–C(2)–C(3)–C(4) | −89.9 | −58.4 | −59.2 | −92.1 | −58.6 | −91.9 | −93.4 |
| C(2)–C(3)–C(4)–C(5) | 69.1 | 6.9 | 6.7 | 65.7 | 6.7 | 66.6 | 71.9 |
| C(3)–C(4)–C(5)–C(6) | 38.1 | 121.2 | 121.0 | 38.5 | 121.8 | 37.4 | 39.9 |
| C(4)–C(5)–C(6)–C(7) | −167.8 | −164.1 | −162.2 | −166.3 | −162.6 | −166.6 | −167.0 |
| C(5)–C(6)–C(7)–C(8) | 116.8 | 94.8 | 96.2 | 123.7 | 94.8 | 123.4 | 114.4 |
| C(6)–C(7)–C(8)–C(9) | −46.8 | −62.4 | −64.5 | −51.8 | −64.0 | −50.6 | −50.0 |
| C(7)–C(8)–C(9)–C(10) | 82.8 | 75.2 | 74.1 | 80.5 | 75.0 | 81.0 | 92.5 |
| C(8)–C(9)–C(10)–C(1) | −133.3 | −130.4 | −128.6 | −127.7 | −129.6 | −128.6 | −140.5 |
| C(9)–C(10)–C(1)–C(2) | 113.9 | 131.2 | 132.5 | 117.5 | 131.9 | 116.7 | 106.5 |
| C(8)–C(7)–C(11)–H(11) | 60.4 | 58.2 | −60.4 | −52.9 | 169.3 | −179.9 | 64.2 |
| C(9)–C(8)–C(7)–C(11) | −169.7 | 175.2 | 169.2 | −178.1 | 171.1 | −176.2 | −174.6 |

[a] Ref. 6. [b] Modified Dale nomenclature. Primes indicate a pseudo-corner ($g^+ g^-$).[20]

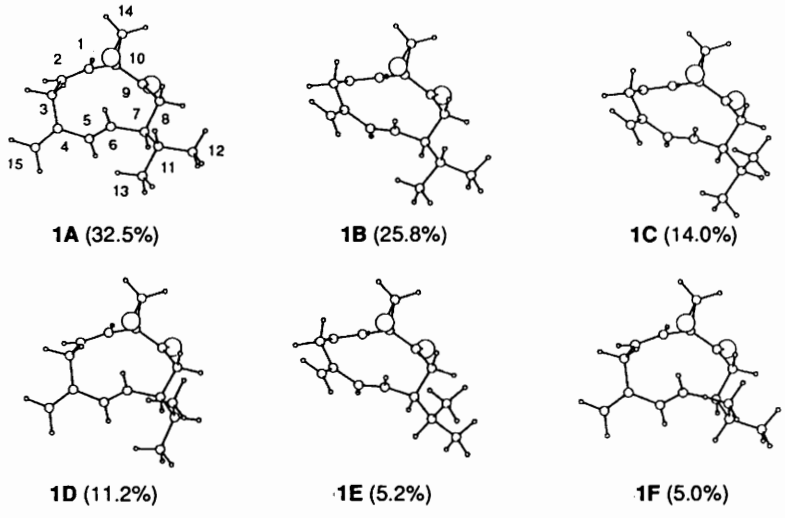


**Fig. 2** Major conformers of periplanone-A **1** (the estimated Boltzmann populations at 298 K in parentheses)

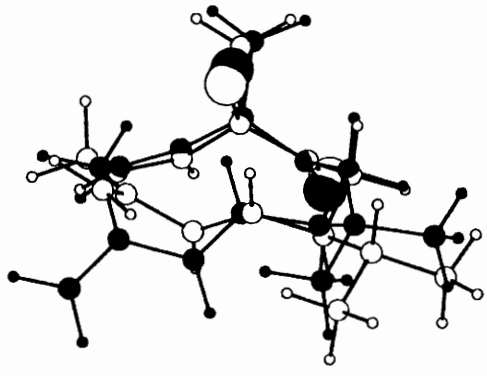

**Fig. 3** Superimposition of global minimum (**1A**, filled) and the second stable conformer (**1B**)

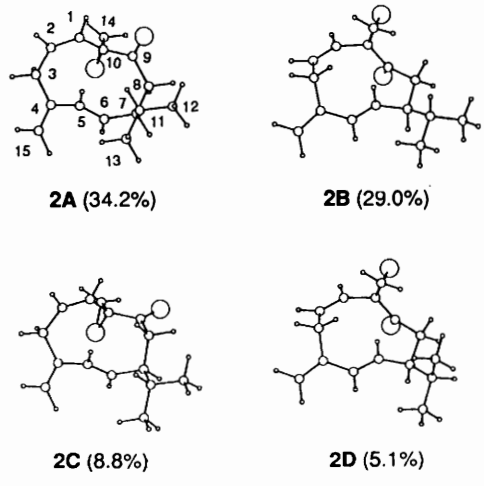


**Fig. 4** Major conformers of the epimer **2** (the estimated Boltzmann populations at 298 K in parentheses)

NMR analysis at 203 K indicated that **3** exists in two dominant conformers with the relative ratio of 2.3:1 (Fig. 8). The calculated ratio of the two major conformers at 203 K based on the relative energies of conformers (2.6:1) is in good agreement with the observed data.

Judging from the verification by NMR analysis of **1**–**3**, our force-field parameters developed in this study are good enough for representing the structural properties of these compounds. For the wider applicability, further examination on these parameters would be necessary.

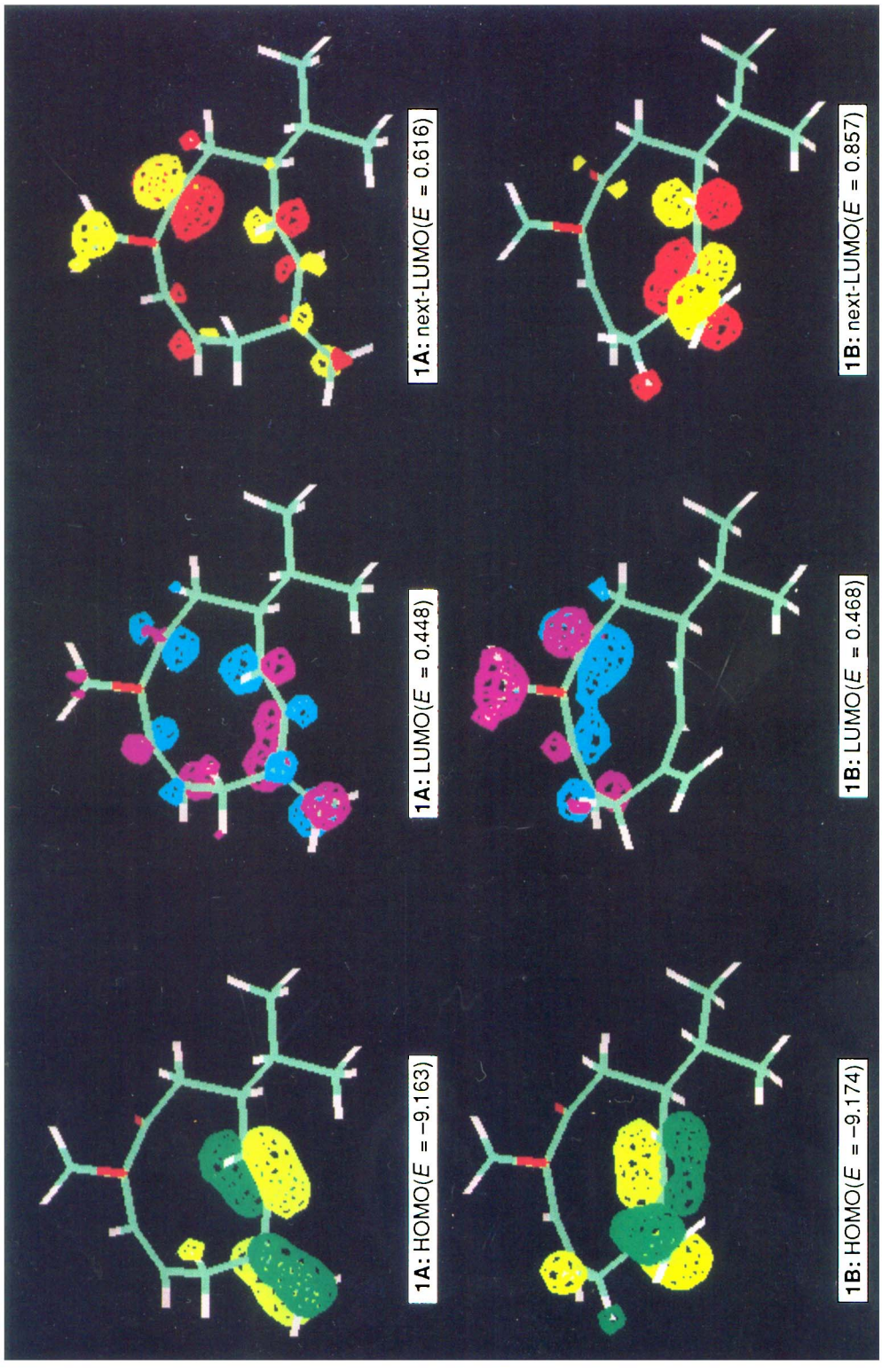


**Fig. 9** Frontier orbitals of the global mimimum and the second stable conformer of **1**; the value of each frontier orbital energy ($E$/eV) is shown in parentheses

Facing p. 1171

**Table 3** Conformational properties of **2**

| | 2A | 2B | 2C | 2D |
|---|---|---|---|---|
| Ring conformations[a] | [14'1'4'] | [1'333'] | [1324] | [1'333'] |
| $\Delta E_S$/kcal mol$^{-1}$ | 0.0 | 0.1 | 0.80 | 1.12 |
| Boltzmann dist. (%) at 25 °C | 34.2 | 29.0 | 8.8 | 5.1 |
| Dihedral angle/° | | | | |
| C(10)–C(1)–C(2)–C(3) | 3.4 | 1.2 | 4.4 | 1.3 |
| C(1)–C(2)–C(3)–C(4) | 56.7 | −90.5 | 57.6 | −92.4 |
| C(2)–C(3)–C(4)–C(5) | −5.7 | 77.5 | 2.7 | 75.4 |
| C(3)–C(4)–C(5)–C(6) | −126.5 | 31.2 | −120.9 | 30.9 |
| C(4)–C(5)–C(6)–C(7) | 162.2 | −165.2 | 162.0 | −164.5 |
| C(5)–C(6)–C(7)–C(8) | −89.4 | 105.6 | −57.7 | 111.5 |
| C(6)–C(7)–C(8)–C(9) | 64.2 | −36.1 | −51.7 | −40.0 |
| C(7)–C(8)–C(9)–C(10) | −78.2 | 90.2 | 76.1 | 89.4 |
| C(8)–C(9)–C(10)–C(1) | 131.3 | −149.1 | 48.6 | −145.6 |
| C(9)–C(10)–C(1)–C(2) | −130.7 | 98.3 | −135.5 | 100.9 |
| C(8)–C(7)–C(11)–H(11) | 59.7 | 59.6 | 59.2 | −51.4 |
| C(9)–C(8)–C(7)–C(11) | −64.2 | −159.5 | −176.5 | −166.8 |

[a] Modified Dale nomenclature. Primes indicate a pseudo-corner ($g^+$ $g^-$).[20] 64 Energy minima were obtained from 456 initial geometries which were generated by CONFLEX2.

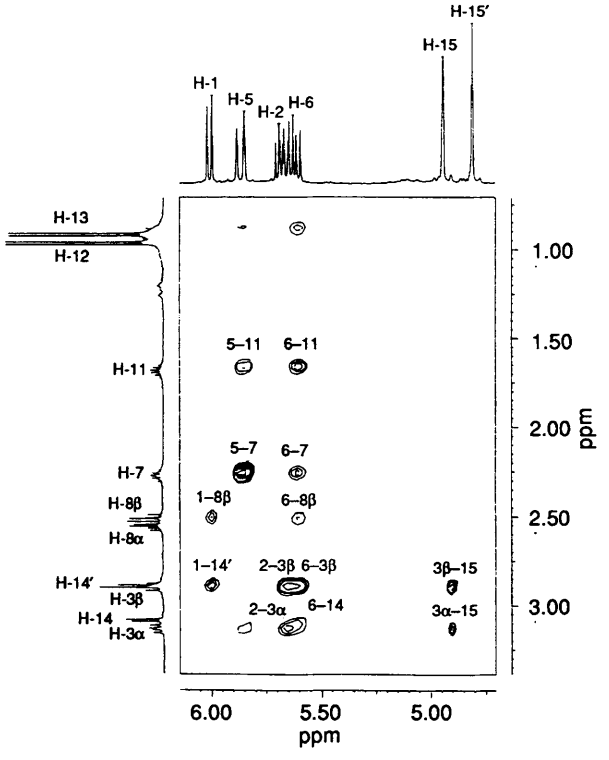


**Fig. 5** Partial 2D NOESY spectrum of **2** (mixing time 3 s) in $CDCl_3$ at 300 K

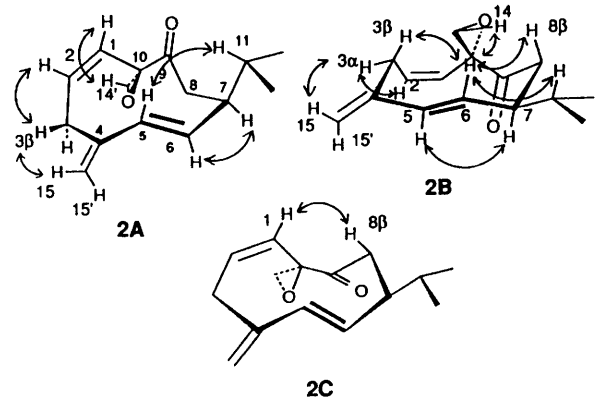


**Fig. 6** Stereostructures of the three major conformers of **2** and intramolecular $^1$H NOE interactions

**Table 4** Conformational properties of **3**

| | 3A | 3B | 3C |
|---|---|---|---|
| Ring conformation[a] | [23'23'] | [123'1'3'] | [232'3'] |
| $\Delta E_S$/kcal mol$^{-1}$ | 0.0 | 0.39 | 1.60 |
| Boltzmann dist. (%) at 25 °C | 62.7 | 32.6 | 4.2 |
| Dihedral angle/° | | | |
| C(10)–C(1)–C(2)–C(3) | −4.4 | −6.0 | −4.6 |
| C(1)–C(2)–C(3)–C(4) | −84.4 | −89.9 | −86.6 |
| C(2)–C(3)–C(4)–C(5) | 69.9 | 53.8 | 64.0 |
| C(3)–C(4)–C(5)–C(6) | −86.1 | 70.5 | −83.5 |
| C(4)–C(5)–C(6)–C(7) | 172.9 | −173.2 | 168.3 |
| C(5)–C(6)–C(7)–C(8) | −75.4 | 100.6 | −116.6 |
| C(6)–C(7)–C(8)–C(9) | −44.1 | −49.3 | 71.0 |
| C(7)–C(8)–C(9)–C(10) | 79.2 | 82.9 | −61.8 |
| C(8)–C(9)–C(10)–C(1) | −114.9 | −133.3 | −40.4 |
| C(9)–C(10)–C(1)–C(2) | 129.5 | 116.9 | 135.2 |

[a] Modified Dale nomenclature. Primes indicate a pseudo-corner ($g^+$ $g^-$ ).[20] Four energy minima were obtained from 27 initial geometries which were generated by CONFLEX2.

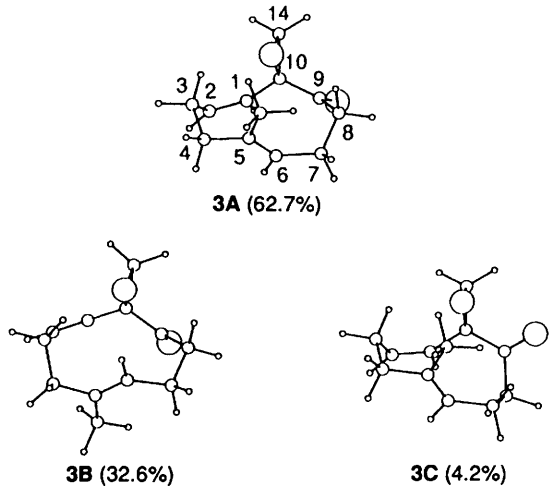


**Fig. 7** Major conformers of analogue **3** (the estimated Boltzmann populations at 298 K in parentheses)

*Molecular Orbital Calculations.—Periplanone-A* (**1**). In Fig. 9, are reproduced the frontier orbital extensions of **1A** and **1B** (orbital energies are shown in parentheses). The highest

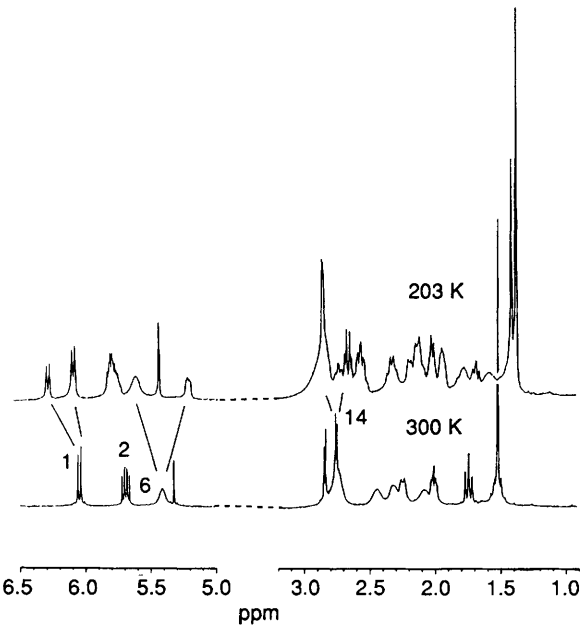


**Fig. 8** Dynamic NMR spectra of **3** in $CD_2Cl_2$ solution at 300 K and 203 K

occupied molecular orbitals (HOMO) of both **1A** and **1B** are localized mainly at the conjugated-diene [C(15)–C(4)–C(5)–C(6)] moiety. Both LUMO and next-LUMO of **1A** are widely distributed over all π-type orbitals of many atoms in the molecule. It may be recalled here that LUMO and next-LUMO of the global minimum of P–B (**4**) are relatively localized. However, a closer analysis revealed that the frontier electron density of the LUMO of **1A** is particularly concentrated at the conjugated-diene; the densities in conjugated-diene, epoxy-carbonyl and double bond moieties are calculated to 1.2316, 0.3018 and 0.3791 ($e^-$ Å$^{-3}$), respectively. The frontier electron density of next-LUMO is more concentrated at the epoxy-carbonyl moiety (1.1027 $e^-$ Å$^{-3}$) than at the conjugated-diene moiety (0.6116 $e^-$ Å$^{-3}$). The same tendency is found in the isopropyl rotamers **1D** and **1F**.

In contrast to **1A**, the LUMO of **1B** (and of the isopropyl rotamers **1C** and **1E**) is mainly localized around the epoxy–carbonyl moiety and the next-LUMO at the conjugated diene moiety (Fig. 9). It is noteworthy that in conformer **1B** the LUMO atomic orbital of the carbonyl carbon is delocalized with that of C(1) olefinic carbon atom, and forms relatively high electron density region along the inner side of the C(9)–C(10)–C(1)–C(2) sequence. A good overlapping between the high density regions around the epoxy-carbonyl moiety of **1A** (next-LUMO) and those of **1B** (LUMO) can be pointed out.

*Epoxy epimer* (**2**). The extension of frontier orbitals of the global minimum (**2A**) and other major conformers except the second and fourth ones (**2B** and **2D**) are quite different from that of **1A**. In the case of **2B**, which possesses essentially the same conformational feature as **1A**, the distribution of frontier orbitals resembles that of **1A**. However, the transposition of the oxygen atom in the epoxy group resulted in the reduction of the delocalization of the π-electrons between the epoxy and carbonyl groups.

*Analogue* (**3**). Among the two major conformers of **3**, the feature of the frontier orbital in the global minimum (**3A**) seems to be similar to that of **5**,[7] while the ring conformation itself is drastically different. On the other hand, the second stable conformer (**3B**) has a **1A** type ring conformation and the LUMO is localized around the epoxy-carbonyl moiety as in the case of the global minimum of **5**. The next-LUMO in **3B** exists

**Table 5** Improved $EF^{(N)}_{(S)}$ obtained by considering two ring types and observed biological activity of compounds

| Compound | Improved $EF^{(N)}_{(S)}$ [a] | Biological activity [b] |
|---|---|---|
| **4** | 3.925 | −13 |
| **5** | 3.011 | −9 |
| **6** | 2.116 | −7 |
| **7** | 1.183 | −6 |
| **8** | 0.865 | −5 |

[a] Effective frontier parameter. [b] $\log_{10}$ [threshold (g)], assessed by behavioural test.

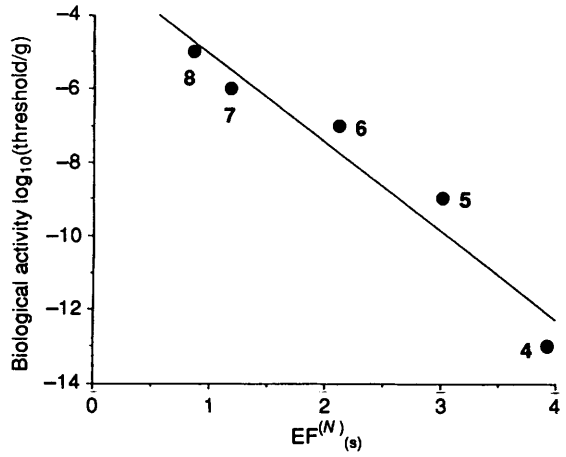


**Fig. 10** Relation between biological activity and the value of improved $EF^{(N)}_{(S)}$ of **4–8**

mainly at the C(1)–C(2) double bond, but the orbital is delocalized around the carbonyl group.

*The Contribution of New Ring Structure as seen in* **1B** *towards the Biological Activity.*—From the results of the MM and MO calculations, the resemblance between the conformational and electronic characteristics of the stable conformers of P–A (**1**) and P–B (**4**)[7] are now apparent. The ring structure and molecular orbital of the global minimum **1A** are superimposable to that of **4**. However, the remarkable difference is the presence of the partially-flapped conformers having the ring type **1B**, of which the combined population (45.0%) is as large as that of **1A** (48.7%). In the case of **4**, the combined population of the conformers having the ring type **1A** is predominant (87.8%), and that of type **1B** is relatively small (6.5%).

In our previous study on structure–activity relationships on **4** and its analogues, only the ring type of the global minimum of **4** had been taken into account as being biologically important. However, good overlapping of frontier unoccupied orbitals around the upper part of the ten-membered ring ($FUMO_{upper}$) are indicated as well as the conservation of their molecular shapes around the biologically important epoxy-carbonyl moiety between **1A** and **1B**, in this study. In the light of the similarity of **1B** to **1A**, it was anticipated that both the ring type of **1A** and **1B** must be biologically relevant ring structures. Therefore, effective frontier parameters [$EF^{(N)}_{(S)}$] were re-calculated for **4–8** with regard to these two ring types (Table 5). As can be seen in Fig. 10, a better correlation between $EF^{(N)}_{(S)}$ values by using the two ring types with the biological activity is obtained as in the following equation.

$$\log_{10}[\text{Activity threshold (g)}] = -2.649 - 2.410 \times EF^{(N)}_{(S)} \quad (5)$$

($R = 0.969$, $\sigma = 0.91$, $F = 45.07$, SE = 0.36, $t_{static} = 6.71$ and $n = 5$)

**Table 6** Population-weighted frontier orbital energy (eV), improved $EF^{(N)}_{(S)}$, observed and predicted biological activity of compounds

| Compound | HOMO/ eV | $FUMO_{lower}$[a]/ eV | $FUMO_{upeer}$[b]/ eV | Improved $EF^{(N)}_{(S)}$[c] | Observed biological activity[d] | Predicted biological activity[d] |
|---|---|---|---|---|---|---|
| **1** | −9.180 | 0.588 | 0.575 | 3.527 | −11 | −11.2 |
| **2** | −9.225 | 0.587 | 0.571 | 1.124 | −7 | −5.4 |
| **3** | −9.385 | 1.126 | 0.574 | 1.070 | > −5 | −5.2 |

[a] Frontier unoccupied orbital around upper part of ten-membered ring. [b] Frontier unoccupied orbital around lower part of ten-membered ring. [c] Effective frontier parameter. [d] $\log_{10}$ [threshold (g)].

The correlation is improved compared to that obtained by using only one ring type ($R = 0.929$).[7]

The biological activities of **1**–**3** are re-calculated from this new linear regression equation (Table 6). The predicted value of biological activity of **1** (threshold: $10^{-11.2}$ g) was in good agreement with that observed in the bioassay. The drastic reduction of the biological activities of **2** and **3** from **1** also agrees with the predicted low values of biological activity. In the case of **2**, however, the observed value is higher than the predicted value. This may be explained by the 0.01% contamination of highly active **1**, which is formed in the synthetics of **2**. The predicted biological activity of **3** means that it has practically no activity in our bioassay system.

## Conclusions

By virtue of the new parameters and CONFEX/MM2 calculations on periplanone-A (**1**), the epoxy epimer (**2**) and the analogue (**3**), their significantly populated conformers have been identified. The validity of the calculated results was confirmed by comparison with X-ray crystallographic and NMR analyses. The global minimum **1A** is well superimposable to that of periplanone-B (**4**). However, the second conformer **1B**, of which the exomethylene functional group is flapped upward is revealed to exist is comparable concentration as **1A** (1:0.92). In contrast, the corresponding ratio in **4** is 1:0.07. The geometries around the epoxy-carbonyl moiety are common between these two ring types. According to the AM1 study, the electronic distributions in the frontier unoccupied orbitals localized around the upper part of the ten-membered ring ($FUMO_{upper}$) of the **1A** type conformers are different from those of **1B**. However the high density regions in $FUMO_{upper}$ are commonly distributed around the epoxy-carbonyl moiety among **1A**, **1B** and the case of **4** (P–B).[7] From these results, the formerly proposed effective frontier parameter $EF^{(N)}_{(S)}$ was re-assessed for the compounds **4**–**8** by taking the two ring types into account, to obtain a better correlation between the improved $EF^{(N)}_{(S)}$ and the biological activity. The calculated value for **1** is in good agreement with that observed in the bioassay. These results show that the conformers with the two ring types as in **1A** and **1B** are equally important to exhibit biological activity. The improved effective frontier parameter $EF^{(N)}_{(S)}$ appears reliable.

In concluding this series of studies, we propose that the frontier unoccupied molecular orbitals localized around the epoxy-carbonyl moiety of periplanones must play an important role for the biological activity. We find no significant linear correlation between biological activities and electronic properties of HOMO and $FUMO_{lower}$, which are mainly located in the conjugated-diene moiety [C(5)–C(6) double bond in **5**] in all compounds examined.[7] However, the contributions of this electron rich region to pheromone recognition in the receptor site cannot be excluded in the view of π–π and hydrophobic interactions. Such discussions may be the subject of future study. As the coupling of computational chemical methods and structure–activity concepts must be potentially powerful, works along this line will provide valuable informations on the recognition of bioactive molecules, and will be linked to design new analogues.

## References


1 H. Hauptmann, G. Mühlbauer and H. Sass, *Tetrahedron Lett.*, 1986, **27**, 6189.
2 S. Kuwahara and K. Mori, *Tetrahedron*, 1990, **46**, 8083, and references cited therein.
3 C. J. Persoons, F. J. Ritter and W. J. Lichtendonk, *Proc. Kon. Ned. Akad. Wetensch. Amsterdam*, 1974, **C77**, 201 (*Chem. Abstr.*, 1974, **81**, 88–209f); for a review on American cockroach sex pheromones, see C. J. Persoons, F. J. Ritter, P. E. J. Verwiel, H. Hauptmann and K. Mori, *Tetrahedron Lett.*, 1990, **31**, 1747, and references cited therein.
4 W. C. Still, *J. Am. Chem. Soc.*, 1979, **101**, 2493.
5 K. Okada, M. Mori, K. Shimazaki and T. Chuman, *J. Chem. Ecol.*, 1991, **17**, 695.
6 M. Mori, K. Okada, K. Shimazaki, T. Chuman, S. Kuwahara, T. Kitahara and K. Mori, *J. Chem. Soc., Perkin Trans. 1*, 1990, 1769.
7 K. Shimazaki, M. Mori, K. Okada, T. Chuman, H. Goto, E. Osawa, K. Sakakibara and M. Hirota, *J. Chem. Soc., Perkin Trans. 2*, 1992, 811.
8 T. L. Macdonald, C. M. Delahunty and J. S. Sawyer, *Heterocycles*, 1987, **25**, 305.
9 T. Harada, T. Takahashi and S. Takahashi, *Tetrahedron Lett.*, 1992, **33**, 369.
10 QCPE #506 AMPAC version 2.1.
11 M. Mori, K. Okada, K. Shimazaki and T. Chuman, *Tetrahedron Lett.*, 1990, **31**, 4037.
12 GAUSSIAN 90, M. J. Frisch, M. Head-Gordon, G. W. Trucks, J. B. Foresman, H. B. Schlegel, K. Raghavachari, M. A. Robb, J. S. Binkley, C. Gonzalez, D. J. Defrees, D. J. Fox, R. A. Whiteside, R. Seeger, C. F. Melius, J. Baker, R. L. Martin, L. R. Kahn, J. J. P. Stewart, S. Topiol and J. A. Pople, Gaussian, Inc., Pittsburgh PA, 1990.
13 K. Sakakibara, H. Kawamura, T. Nagata, M. Hirota, K. Shimazaki and T. Chuman, submitted.
14 U. Burkert and N. L. Allinger, *Molecular Mechanics*, ACS Monograph 177, American Chemical Society, Washington, DC, 1982.
15 H. Gotō and E. Ōsawa, *J. Chem. Soc., Perkin Trans. 2*, 1993, 187.
16 H. Gotō and E. Ōsawa, *Tetrahedron*, 1993, **49**, 387.
17 C. A. G. Haasnoot, F. A. A. M. de Leeuw and C. Altona, *Tetrahedron*, 1980, **36**, 2783.
18 S. Masamune, P. Ma, R. E. Moore, T. Fujiyoshi, C. Jaime and E. Ōsawa, *J. Chem. Soc., Chem. Commun.*, 1986, 261.
19 E. Ōsawa, T. Ouchi, N. Saito, M. Yamato, O. S. Lee and M.-K. Seo, *Org. Magn. Reson.*, 1992, **30**, 1104.
20 H. Gotō, *Tetrahedron*, 1992, **48**, 7131.


*Paper* 3/00371J
*Received* 20*th January* 1993
*Accepted* 23*rd February* 1993